Astrocytic abnormalities and global DNA methylation patterns in depression and suicide

ARTICLE *in* MOLECULAR PSYCHIATRY · MARCH 2014

Impact Factor: 14.5 · DOI: 10.1038/mp.2014.21 · Source: PubMed

7 AUTHORS, INCLUDING:

Corina Nagy
McGill University
10 PUBLICATIONS **79** CITATIONS
SEE PROFILE

Matthew Suderman
University of Bristol
73 PUBLICATIONS **1,355** CITATIONS
SEE PROFILE

Moshe Szyf
McGill University
298 PUBLICATIONS **18,184** CITATIONS
SEE PROFILE

Naguib Mechawar
McGill University
75 PUBLICATIONS **2,058** CITATIONS
SEE PROFILE

Molecular Psychiatry (2014), 1–9

www.nature.com/mp

ORIGINAL ARTICLE

Astrocytic abnormalities and global DNA methylation patterns in depression and suicide

C Nagy[1,2], M Suderman[3,4], J Yang[1], M Szyf[4,5], N Mechawar[1,2,6], C Ernst[1,6] and G Turecki[1,2,6]

Astrocytes are glial cells specific to the central nervous system and involved in numerous brain functions, including regulation of synaptic transmission and of immune reactions. There is mounting evidence suggesting astrocytic dysfunction in psychopathologies such as major depression, however, little is known about the underlying etiological mechanisms. Here we report a two-stage study investigating genome-wide DNA methylation associated with astrocytic markers in depressive psychopathology. We first characterized prefrontal cortex samples from 121 individuals (76 who died during a depressive episode and 45 healthy controls) for the astrocytic markers *GFAP, ALDH1L1*, *SOX9, GLUL, SCL1A3, GJA1* and *GJB6*. A subset of 22 cases with consistently downregulated astrocytic markers was then compared with 17 matched controls using methylation binding domain-2 (MBD2) sequencing followed by validation with high-resolution melting and bisulfite Sanger sequencing. With these data, we generated a genome-wide methylation map unique to altered astrocyte-associated depressive psychopathology. The map revealed differentially methylated regions (DMRs) between cases and controls, the majority of which displayed reduced methylation levels in cases. Among intragenic DMRs, those found in GRIK2 (glutamate receptor, ionotropic kainate 2) and BEGAIN (brain-enriched guanylate kinase-associated protein) were most significant and also showed significant correlations with gene expression. Cell-sorted fractions were investigated and demonstrated an important non-neuronal contribution of methylation status in *BEGAIN*. Functional cell assays revealed promoter and enhancer-like properties in this region that were markedly decreased by methylation. Furthermore, a large number of our DMRs overlapped known Encyclopedia of DNA elements (ENCODE)-identified regulatory elements. Taken together, our data indicate significant differences in the methylation patterns specific to astrocytic dysfunction associated with depressive psychopathology, providing a potential framework for better understanding this disease phenotype.

Molecular Psychiatry advance online publication, 25 March 2014; doi:10.1038/mp.2014.21

INTRODUCTION

Glial cells account for at least 75% of brain cells[1] and are implicated in a range of psychiatric disorders, including alcoholism,[2] schizophrenia,[3] depression[4] and suicide.[5,6] In particular, astrocytic dysfunction is evident in depressive psychopathologies including suicide.[4] Astrocytes are multifaceted cells with numerous functions, including regulation of blood flow, synaptic communication and plasticity, immune regulation[7] and maintenance of neuronal functioning.[8] These—and other—physiological roles are likely to have an impact in depression and suicide, given evidence from postmortem and animal studies showing altered astrocytic morphologies[5] and persistently decreased expression of astrocyte-specific genes such as glial fibrillary acidic protein (GFAP),[9] glutamine synthetase (GLUL),[10] the glial high-affinity transporters, SLC1A2 and SLC1A3,[10] aquaporin 4 (ref. 11) and the connexin genes such as Cx30 and Cx43.[6]

Despite consistent reports, little is known about the underlying etiological mechanisms linking astrocytic dysfunction to depression and suicide. These could involve epigenetic factors such as DNA methylation that stably modulates gene expression. Indeed, DNA methylation changes at specific genomic loci are associated with increased risk of psychopathology.[12,13] The purpose of the current study was to identify DNA methylation patterns associated with astrocytic alterations in depression and suicide. To this end, we characterized expression of astrocytic markers *GFAP, ALDH1L1, SLC1A3, GJA1, GJB6*, *GLUL* and *SOX9* in the dorsolateral prefrontal cortex (PFC) of individuals having died by suicide and sudden death controls. For all subjects with consistent and pronounced downregulation of astrocytic markers, we conducted methylation binding domain-2 (MBD2) enrichment coupled with next-generation sequencing. Our results suggest a framework to better understand how astrocyte dysfunction impacts depression and suicide.

MATERIALS AND METHODS

Brain samples, clinical characterization and group composition

Brain tissue was obtained from the Douglas-Bell Canada Brain Bank (DBCBB; http://www.douglas.qc.ca/page/brain-bank). The DBCBB recruits suicide cases and sudden death control subjects. To avoid prolonged agonal states, both cases and controls recruited to the bank cannot undergo resuscitation procedures or medical intervention. Brain tissue for the DBCBB is collected after consent is obtained from next-of-kin. Families are recontacted after ~4 months to undergo a series of structured

[1]McGill Group for Suicide Studies, Douglas Mental Health University Institute, McGill University, Montreal, QC, Canada; [2]Integrated Program in Neuroscience, McGill University, Montreal, QC, Canada; [3]McGill Centre for Bioinformatics, McGill University, Montreal, QC, Canada; [4]Sackler Program for Epigenetics and Developmental Psychobiology, McGill University, Montreal, QC, Canada; [5]Department of Pharmacology and Therapeutics, McGill University, Montreal, QC, Canada and [6]Department of Psychiatry, McGill University, Montreal, QC, Canada. Correspondence: Dr G Turecki, McGill Group for Suicide Studies, Douglas Mental Health University Institute, McGill University, 6875 Lasalle Boulevard, Montreal, QC, Canada H4H 1R3.
E-mail: gustavo.turecki@mcgill.ca
Received 22 May 2013; revised 13 January 2014; accepted 31 January 2014

interviews, known as psychological autopsies, with the person best acquainted with the deceased, as described elsewhere.[14] Interviews are supplemented with information from archival material obtained from hospitals, the Coroner's office or social services. Following the interviews, clinical vignettes are produced and assessed by a panel of clinicians to generate Diagnostic and Statistical Manual of Mental Disorders-IV diagnoses. This is a well-accepted and valid procedure to obtain clinical information on deceased individuals through proxy-based interviews.[15,16]

Cases in this study were individuals who died by suicide as determined by the coroner and following psychological autopsies met the criteria for major depressive disorder or had no axis I, but with evidence of depressive symptoms at the moment of death. Controls were individuals who died suddenly in motor vehicle accidents or by cardiac arrest and did not have evidence of axis I disorders. For preliminary screening, we included 121 brain samples (76 cases) and tested two cortical brain regions. Low expressors were identified using tissue from Brodmann area 10 and then replicated in tissue from Brodmann area 8/9. Only tissue from the left hemisphere (gray matter only) was used. These cortical regions are consistently implicated in depression[17–20] and are involved in higher order functioning such as decision making, which is impaired in suicide.[21]

The second part of this study used expression profiles to define the case group. Specifically, at least 5/7 genes investigated had to be in the lowest quartile ($n = 22$) of expression (Supplementary Figure 1–3). Controls were selected on the basis of age, gender and post mortem interval to group-match the suicide group; gene expression was not used to select controls. The average post mortem interval (± s.e.m.) for controls was 18.8 (±2.91) and for cases was 17.7 (±4.48). The average age of controls was 41.3 (±5.87) and for suicides was 41.0 (±2.64); and the average RNA integrity number for controls was 6.2 (±0.16) and for suicides was 6.4 (±0.16). There was no significant difference between groups for any of these variables. This study was approved by the Douglas Institute Research Ethics Board.

Methods for histological sectioning, gene expression analysis, MBD protein sequencing (MBD2-seq), sequencing analysis, Encyclopedia of DNA elements (ENCODE) analysis, high-resolution melting and site-specific bisulfite sequencing, fluorescence activated cell sorting (FACS) and functional cell assays can be found in the online Supplementary Information (Supplementary Methods).

RESULTS

Identification of cases with low expression of astrocyte-related genes

To identify subjects with potential astrocytic dysfunction, we screened PFC samples obtained from the DBCBB for expression levels of genes exclusively or primarily expressed in astrocytes. This initial screen was conducted on 121 subjects (87 males), including 76 individuals who died by suicide, and 45 sudden death controls. We selected the following seven genes for screening based on their high expression in astrocytes: *GFAP*, *ALDH1L1*, *SOX9*, *GLUL*, *SCL1A3*, *GJA1* and *GJB6,* all showing significantly decreased expression in cases compared with controls (Figure 1). To demonstrate that these results specifically reflected a decrease in astrocyte gene expression, we examined the level of NeuN (a.k.a. *RBFOX3*), a well-known marker of neurons [22] and found no significant difference between cases and controls (Figure 1h).

Epigenetic factors are known to regulate gene expression and may contribute to the astrocytic dysfunction observed in our cases. Specifically, we hypothesized that DNA methylation patterns differ between groups. To test this, we conducted a genome-wide methylation sequencing study focusing on individuals with the most severe molecular phenotype. We selected cases showing the lowest mRNA expression levels of the astrocyte marker genes used for screening, and operationally defined extreme cases by expression levels in the bottom quartile for at least 5/7 genes; 22 cases met these criteria (Supplementary Figure 1–5; and Supplementary Tables 1 and 2). Cases were compared with 17 psychiatrically normal controls grouped-matched according to age, RNA integrity number, post mortem interval and gender. To decrease variability, all subjects included in the analysis were males.

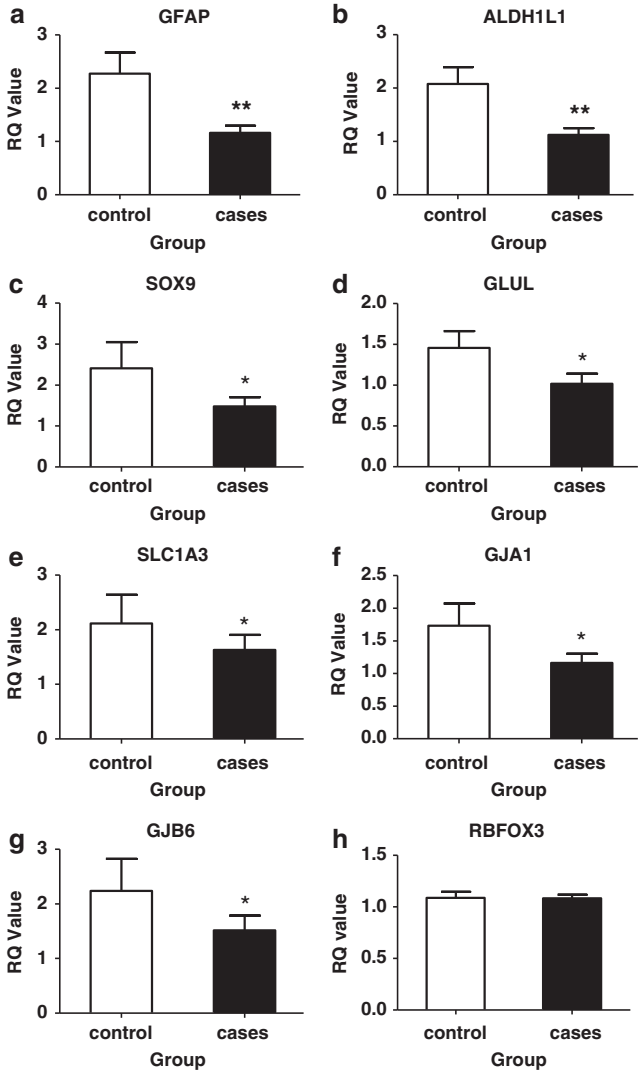

Figure 1. Quantitative PCR screening of 76 cases and 45 controls for astrocytic genes showed a strong decrease in expression of astrocyte markers in Brodmann area 10. (**a**) GFAP; (mean ± s.e.m.), case (1.17 ± 0.13), control (2.27 ± 0.40), $P = 0.0068$; (**b**) ALDH1L1, case (1.12 ± 0.13), control (2.08 ± 0.31), $P = 0.0023$; (**c**) SOX9, case (1.48 ± 0.22), control (2.41 ± 0.64), $P = 0.03$; (**d**) GLUL, case (1.02 ± 0.12), control (1.46 ± 0.21), $P = 0.01$; (**e**) SCL1A3, case (1.63 ± 0.28), control (2.12 ± 0.52), $P = 0.04$; (**f**) GJA1, case (1.17 ± 0.14), $P = 0.03$; (**g**) GJB6, case (1.48 ± 0.23), control (2.41 ± 0.64), $P = 0.05$; (**h**) expression of RBFOX3 (a.k.a. NeuN, a standard marker for mature neuronal identity) shows no difference between groups ($P = 0.86$). (Tests performed were either Student's *t*-test or Mann–Whitney U-test, depending on the distribution of the data). $^{*}P \leq 0.05$; $^{**}P \leq 0.001$.

Generation of high-quality genome-wide MBD2-seq profiles

We performed genome-wide DNA methylation analysis by isolating fragmented DNA using biotinylated-MBD2. The MBD2 protein specifically targets densely methylated CpGs[23] and does not target hydroxymethylated cytosines,[23,24] thus sequencing MBD2-enriched DNA identifies methylated regions from the whole genome. Comparing the number of sequenced reads matching each region enabled us to identify methylation differences between cases and controls. Many quality control steps where preformed to insure high quality (Supplementary Figures 6 and 7; and Supplementary Table 3).

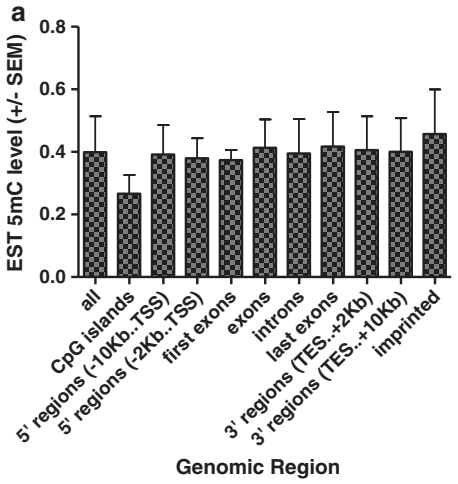

b

Genomic region of DMR	% of DMRs (115)
first exon	0.87%
exon	2.61%
gene	33.91%
intron	31.30%
-5000bp..TSS	10.43%
TES..+5000bp	6.09%
Intergenic	56.52%

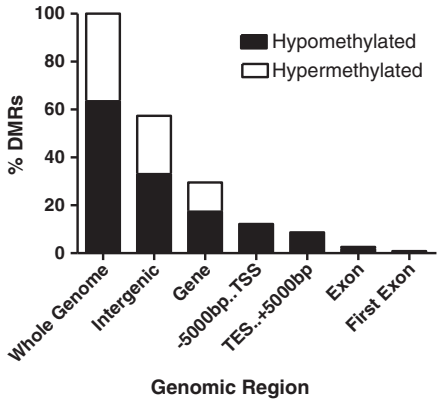

Figure 2. Estimated methylation levels across the genome and level of methylation in case relative to controls. (**a**) Comparison of DNA methylation levels between cases and controls reveals region-specific effects in the human genome. The overall methylation levels were estimated from region read counts. The Wilcoxin rank-sum test was used to determine significance of methylation differences between pairs of region types. Only introns were not different than 3′ regions, all other pairs of region types were significantly differentially methylated ($P < 2E10–22$). EST, estimated; TSS, transcription start site; TES, transcription end site; imprinted genes are based on geneimprint.com; CpG islands are defined as regions with an expected CpG frequency of >60%, a GC content >50% and a length >200 bp. (**b**) The percentage summary of DMRs in known genome regions. (**c**) Cases with decreased expression of astrocyte-associated genes show a genome-wide pattern of hypomethylation. 63.5% of DMRs were hypomethylated in cases compared with controls.

In total, we obtained nearly 450 million reads, and mean read counts were similar between groups (Student's *t*-test, $P = 0.85$) (Supplementary Table 4). Our reads provided 20x coverage per base for the MBD enrichment (Supplementary Figure 8). We assessed our data for genomic metrics, irrespective of disease status. First, we assessed the consistency of sequencing data by measuring overall methylation levels at specific genomic features. DNA methylation levels were consistent with expectations at all genomic loci assessed: CpG islands showed the least amount of methylation, first exons showed less methylation than other exons and imprinted regions showed increased levels of methylation (Figure 2a; Wilcoxin rank-sum, $P < 2E10–22$).

Second, to validate the enrichment of methylated reads and to confirm bioinformatic processing, we selected regions of the genome identified in sequencing data as either highly methylated or poorly methylated and re-performed MBD2 enrichment reactions using identical DNA samples as the initial sequencing reaction. We found that levels identified as highly methylated in the sequencing reaction gave the lowest Ct values in quantitative real time-PCR analysis, and the opposite was found in genomic regions with low methylation (region 1: $r = -0.81$, $t = 0.025$; region 2 $r = -0.74$, $t = 0.047$; and region 3: $r = -0.61$, $t = 0.09$) (Supplementary Figure 9).

Differentially methylated regions in cases and controls

After ensuring quality and accuracy of MBD2 enrichment, we assessed case and control group differences. There were 115 differentially methylated regions (DMRs) across the genome. Of these, 33.91% ($N = 34$) were found in genes, almost all intragenic and falling within introns ($N = 31$; 31.3%). Nearly 11% ($N = 14$) of DMRs were within promoters, defined as sequences up to 5 kb upstream of transcription start sites (Figure 2b). However, the majority of DMRs were found in intergenic regions 56.6% ($N = 66$).

As expected, the number of reads mapping back to each chromosome strongly correlated with their size (Spearman $r = 0.83$, $P < 0.0001$), while there was no difference in the contribution of each group to chromosome coverage (Supplementary Figures 10a and b). We found no relationship between chromosome size and location of DMR, that is, DMRs were independent of size and read count (Spearman $r = -0.15$, $P = 0.48$) (Supplementary Figure 10c).

Most DMRs were hypomethylated in cases. There was considerable decrease in methylation within the gene body of cases; 58.8% of the within gene DMRs were less methylated in cases compared with controls, and these results were consistent in the intergenic regions, where a similar percentage of DMRs were hypomethylated (57.6%; Figure 2c).

We observed two genomic regions enriched with DMRs clusters: one on chromosome 10 and another on the X chromosome (Fisher's exact test, FDR < 0.05; Supplementary Table 5; and Supplementary Figure 11). The DMRs in these two regions overlapped strongly with ENCODE elements suggesting potentially important regulatory roles.[25]

Functional relevance of DMRs derived from ENCODE data

Using publically available data from the ENCODE, we performed an *in silico* assessment of the regulatory potential of each DMR by identifying overlaps with ENCODE features. Altogether, we assessed 41 ENCODE features that include histone modifications and DNA-binding proteins known to influence gene transcription. Our analysis showed enrichment for 37 of the 41 features in hypomethylated regions (Fisher's exact test average $P < 4.82E–03$; Supplementary Table 6); however, there was no enrichment in hypermethylated sites. Nearly half the DMRs contained at least one ENCODE feature (Figure 3a). Histone 3 lysine 4 trimethylation (H3K4me3), a chromatin modification enriched in gene promoters and most often associated with euchromatin and active transcription,[26] and DNase I hypersensitivity sites (DHSs) that are associated with many *cis*-regulatory elements including promoters, enhancers, insulators, silencers and locus control regions,[27] overlapped most frequently with the DMRs (Figure 3b). Both features overlapped with 22.6% of DMRs. As DHSs have been shown to precede promoter regions marked by H3K4me3,[27] it was not surprising that most DHS sites overlapped with H3K4me3. We found four DMRs with an impressive overlap of 20 or more ENCODE features. These regions were found in the pericentromeric region of four different chromosomes (4, 7, 16 and 21). One of the most conserved functions of DNA methylation is stabilizing

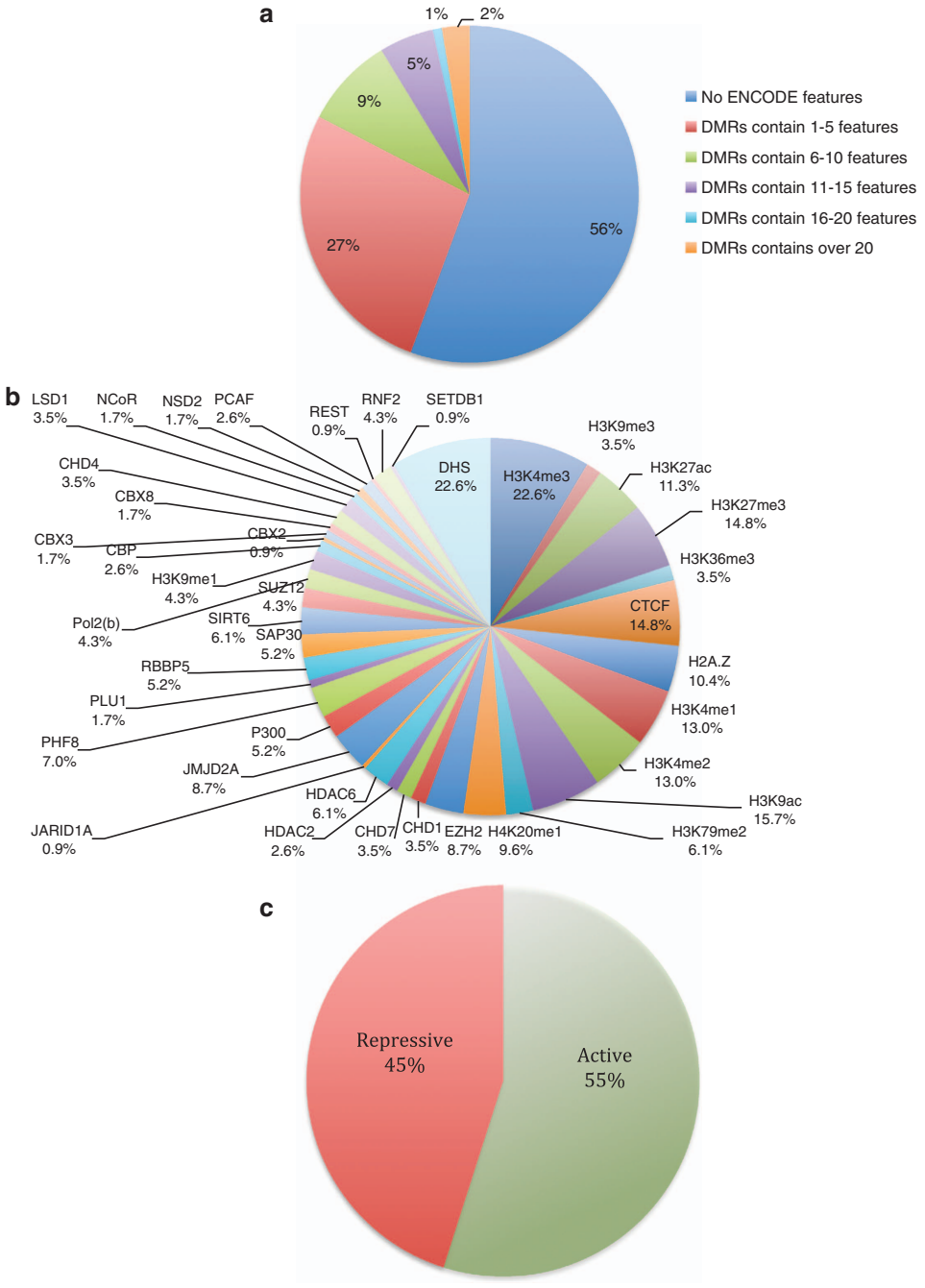

Figure 3. Differentially methylated regions (DMRs) overlap with Encyclopedia of DNA elements (ENCODE) data. (**a**) The breakdown of DMRs overlapping multiple ENCODE feature showing 44% of DMRs overlapped with at least one ENCODE feature. (**b**) The proportion of all queried regulatory features represented within our sample. (**c**) The breakdown of DMRs overlapping with active or repressive regulatory marks.

pericentromeric repeats by inhibiting their latent transcriptional potential.[28] Moreover, decondensing of these heterochromatic regions can result in illegitimate rearrangements,[29] therefore hypomethylation in these regions often lead to notable consequences.

To assess the permissive or inhibitory relationship of the ENCODE data with our data, we grouped the ENCODE features into active or repressive marks based on their known function (Supplementary Tables 6–8). The distribution of DMRs falling into each category was comparable, with 45% overlapping repressive elements and 55% overlapping active elements (Figure 3c).

Differentially methylated astrocytic genes

As our subjects were selected based on astrocytic expression patterns, we were interested in potential associations between DMRs and astrocyte and/or astrocyte-regulatory genes. To assess whether these genes were associated with DMRs, we conducted gene ontology analyses focusing on genes highly expressed in astrocytes and genes coding for regulatory factors of astrocytic expression. There were four astrocyte-associated genes coded within regions of differential methylation (Table 1), containing multiple sites of differential methylation. These represented 21% of the gene-associated DMRs.

Table 1. The list of astrocyte-associated genes within the data set

Chr	*Gene name*	*Meth status*	*ENCODE overlap*	*Regions*	*Strand*	*Avg Log_2 fold change*	*Avg adj P-value*	*No. of win*	*Function*
6	*GRIK2*	↓	None	Intronic	+	1.44	0.09	2	Glutamate ionotropic kianate receptor
10	*NEBL*	↓	None	Intronic	–	2.00	0.11	2	Actin binding-related protein
3	*PVRL3*	↑	None	Intronic	+	2.96	0.08	1	Adhesion molecule at adhesion junctions
[a]3	ROPN1B	↑	Both	Downstream of TES	–	1.04	0.01	2	Signal transduction

Abbreviations: Adj, adjusted; Avg, average; ENCODE, Encyclopedia of DNA elements; TES, transcription end site. These genes were selected based on functions such as cation homeostasis, response to oxidative stress and glutamatergic synaptic transmission. Genes were supplemented by the addition of genes described by Cahoy *et al.*[30] as enriched in astrocytes. Some genes have multiple windows of methylation differences; altogether, this list represents seven DMRs of the previously described 34 gene-based DMRs (~21%). 'Meth status' refers to whether the regions show an increase (↑) or decrease (↓) in methylation. 'ENCODE overlap' refers to either DHS or H3K4me3, both or no overlap with the DMR. 'Region' describes the general genomic region where the DMR is found for that gene. 'Strand' refers to the location of the genes, either on the sense (+) or antisense (–) strand. 'Avg log_2 fold change' is the absolute difference of methylation at that site, it is averaged to account for the multiple windows (DMRs) found in the gene. 'Avg adj *P*-value' is the significance of the fold change adjusted to correct for multiple testing, averaged as before. 'No. of win' is the number of windows found within that gene; a window represents a DMR. 'Function' is a brief functional description of the gene. The list is ranked by DMR containing windows, and then lowest Avg adj *P*-value and Avg log_2 fold change. [a]This DMR is technically not in the primary variant of *ROPN18*.

Gene-specific validation of DMRs showed inverse correlation to gene expression levels

We validated the most significant DMRs, focusing on the DMRs related to astrocytic function (Table 1) and the complete intragenic DMRs (Supplementary Table 10). These DMRs were, respectively, in *GRIK2* (glutamate receptor, ionotropic kainate 2) and *BEGAIN* (brain-enriched guanylate kinase-associated protein; Figures 4a and b). *GRIK2* is implicated in astrocytic function and has been associated with mood disorders,[30–33] whereas *BEGAIN* is associated with cellular communication.[34] For validation, we performed both bisulfite cloning (Bs-Cloning) and high-resolution melting (HRM) analysis. In both cases, DMRs were consistent with the MBD2-seq analysis, though as expected, HRM showed less sensitivity. HRM results are presented in Figures 4c and g, and show significant differences for both GRIK2 (Student's *t*-test, $P = 0.02$) and *BEGAIN* (Student's *t*-test, $P = 0.007$) in the same direction observed with the MBD2-seq data. With Bs-cloning, we achieved base-pair resolution of methylation levels for *GRIK2* and *BEGAIN,* which strongly supported the MBD2-seq data. (Figures 4d and h; and Supplementary Tables 9a and b). Next, we measured expression levels for each gene, finding an increase in *GRIK2* expression in cases (Figure 4e; $P = 0.012$). For *BEGAIN,* there are two major transcripts with little known about their expression patterns. We investigated brain and peripheral tissues, and found that variant 1 has increased expression in the brain (Figure 4j). When we assessed expression of *BEGAIN* transcripts, we observed a marked decrease of variant 1 in cases (2.3-fold decrease, $P < 0.0001$), whereas variant 2 remained unchanged (Figures 4k and l). Analysis of cluster CpGs methylation and expression showed a significant inverse correlation for both *GRIK2* (Figure 4f, $r = -0.37$, $P < 0.05$) and *BEGAIN* (Figure 4m, $r = -0.37$, $P < 0.05$), suggesting a role for methylation regulating expression in these genes.

Non-neuronal cells from case samples drive methylation difference in *BEGAIN*

As DNA methylation is known to be cell-type specific, we used FACS to separate tissue homogenates into neuronal and non-neuronal fractions. Although it is currently methodologically challenging to isolate astrocytic fractions from frozen tissue, the non-neuronal fraction is primarily composed of astrocytes as they make up the bulk of non-neuronal cells of the human brain. We collected nuclei marked with NeuN and unmarked nuclei for all samples. DNA from each fraction was directly bisulfite converted, then subjected to cloning and Sanger sequencing as for validation of brain homogenates. For *GRIK2,* we observed no difference in methylation across cell types (Supplementary Figure 14d), however, for *BEGAIN* we observed a marked increase of methylation for cases in the non-neuronal fraction, suggesting that the sizeable difference in methylation between cases and controls was largely driven by non-neuronal cells (Figure 4i; one-way analysis of variance (ANOVA); $F(3,32) = 10.74$, $P < 0.0001$).

DNA methylation in DMR represses transcription

Considering the strong increase of methylation detected in both the homogenate and non-neuronal cellular fraction of BEGAIN, we decided to assess this region in a functional cell assay to determine the direct consequences of methylation. As suggested by the CHROMHMM from ENCODE (Supplementary Figure 15), this region of *BEGAIN* has both promoter and enhancer capabilities, therefore the 474-bp amplicon was inserted into two separate CpG-free vectors, one containing no endogenous promoter (Figure 5a) to test potential promoter activity and a second under the control of the human EF-1α promoter to test enhancer-like activity (Figure 5b). The inserted amplicons were either fully methylated or fully unmethylated, the report assays were performed in quintuplicate and repeated twice independently. This 474-bp region of *BEGAIN* clearly showed promoter activity that was fully repressed by methylation (Figure 5c; Kruskal–Wallis = 19.94, d.f., 3, $P < 0.0001$; Supplementary Figures 15a and b). Equally, when this region of *BEGAIN* was inserted in an enhancer position next to the human EF-1α promoter, methylation caused complete loss of reporter gene expression (Figure 5d; Kruskal–Wallis = 22.15, d.f., 3, $P < 0.0001$; Supplementary Figures 15c and d). These results indicate a potent effect of DNA methylation on this region of BEGAIN and suggest a potentially causative role of methylation in the downregulation of the *BEGAIN* variant 1 that we observed in cases with astrocytic dysfunction.

DISCUSSION

In this study, we investigated genomic DNA methylation patterns that may contribute to astrocyte dysfunction in depression and suicide. First, we characterized groups for their expression profile of several astrocyte-associated genes in the PFC. Subsequently, we conducted MBD2-seq focusing on cases with clear astrocytic dysfunction at a molecular level. The profiles generated in our study revealed differential DNA methylation at multiple loci, including ENCODE-associated regulatory sequences. In following-up our top intragenic DMRs, we were able to replicate our findings

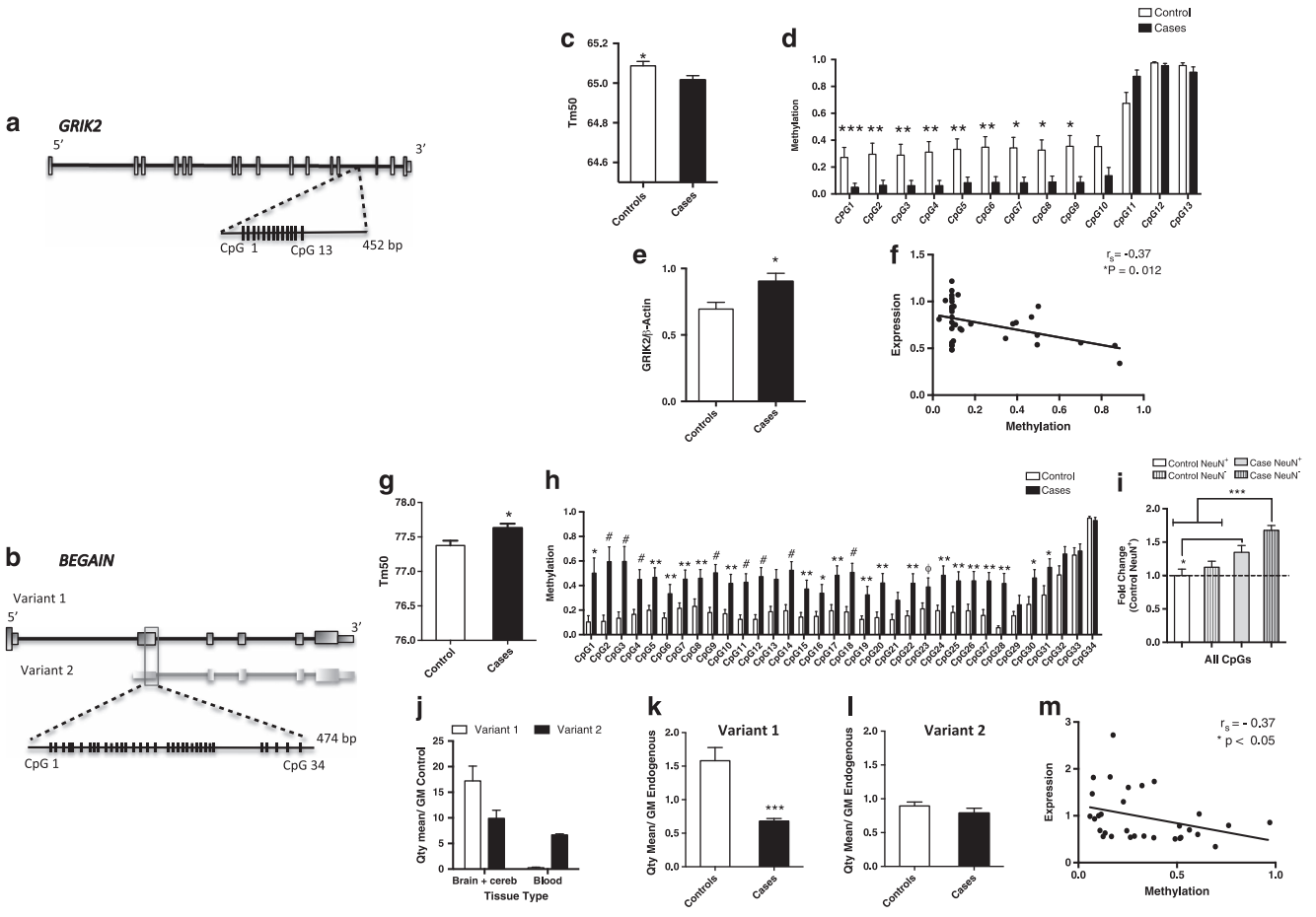

Figure 4. Gene-specific validation of differentially methylated regions (DMRs) shows inverse correlation to gene expression levels, and fluorescence activated cell sorting (FACS) shows specific non-neuronal contribution. Schematic diagrams of each gene highlighting region of methylation difference, the size of amplicon and the number and distribution of CpGs for each (**a**) *GRIK2* and (**b**) *BEGAIN*, respectively. (**c**) High-resolution melting (HRM) results for GRIK2 that show a decreased methylation in cases (unpaired *t*-test, $^*P = 0.025$). (**d**) Bs-cloning supports MBD-seq and HRM results showing a cluster of the first nine CpGs as significantly less methylated in cases ($n = 21$, average 17 clones per sample) than controls ($n = 20$, average 17 clones per sample) mixed model regression analysis was perform to assess significance of methylation at each CpG, $^*P < 0.05$, $^{**}P < 0.01$, $^{***}P < 0.001$ exact values for pairwise comparison are in Supplementary Table 9a and cluster analysis in Supplementary Table 9b). (**e**) *GRIK2* expression as measured by relative quantitation using TAQMAN probes shows an increasing in expression in cases (Student's *t*-test, $^*P = 0.012$). (**f**) GRIK2 expression correlates with the cluster of significantly differentially methylated CpGs (average methylation at each CpG, Spearman $r = -0.37$, $^*P = 0.012$). (**g**) HRM results for *BEGAIN* show more methylation in cases compared with controls with (unpaired *t*-test with Welch's correction, $^{**}P = 0.007$). (**h**) Bs-cloning for BEGAIN shows striking increase in methylation of cases ($n = 17$, average 11 clones per sample) compared with controls ($n = 18$, average 11 clones per sample) mixed model regression analysis was perform to assess significance of methylation at each CpG; $^*P < 0.05$, $^{**}P < 0.01$, $^{\#}P < 0.00$, ϕ trend 0.053, exact values for pairwise comparison are in Supplementary Table 9c and cluster analysis in 9d). Cases showed on average a threefold increase in methylation within cluster on *BEGAIN*. (**i**) *BEGAIN* FACS samples show a strong contribution of methylation from the non-neuronal cell fraction in case samples, whereas there is no difference in controls sample methylation between the two fractions ($n = 9$ for all groups, average 17 clones per sample, one-way ANOVA $F(3.32) = 10.74$, $P < 0.0001$, Tukey's *post hoc*, $^*P < 0.05$, $^{***}P < 0.001$). (**j**) Analysis of *BEGAIN* variant expression in brain and blood. Experiment was independently repeated three times with two endogeneous controls per experiment, geometric mean of endogenous control was calculated and expression was normalized to this value. We qualitatively show that variant 1 is more expressed in brain and almost not present in blood, while we still detect variant 2 in blood. (**k**) The astrocytic dyfunction group show a 2.3-fold decrease in the expression of *BEGAIN* variant 1 compared with controls (Mann–Whitney U-test; $P < 0.0001$), (**l**) whereas variant 2 shows no change (Student's *t*-test, $P = 0.26$). (**m**) The decrease in variant 1 expression correlates with the significantly differentially methylated cluster of CpGs in *BEGAIN* (average methylation at each CpG, Spearman $r = -0.37$, $^*P = 0.019$).

using two independent techniques, and in addition, we found that the methylation differences correlated with gene expression changes. Furthermore, we demonstrated that in cases, non-neuronal cells drive methylation changes observed in *BEGAIN*. Finally, we showed through functional cell assays that methylation of our isolated region in *BEGAIN* almost completely abolishes reporter gene expression *in vitro*. This is, to our knowledge, the first study using next-generation sequencing to investigate genome-wide differential methylation associated with depression and suicide.

Most DNA methylation studies use candidate approaches; among the strengths of the current study is the genome-wide approach coupled by DNA sequencing. Studies in rats and humans have shown discrete regions of hypermethylation associated with behavioral phenotypes and transcriptional regulation.[35,36] These studies used candidate gene approaches or were focused on promoter sequences.[37] In the present study, we avoided restricting our analyses to promoter regions, and provided an unbiased view of DNA methylation associated with depressive psychopathology and suicide. About 90% of the DMRs

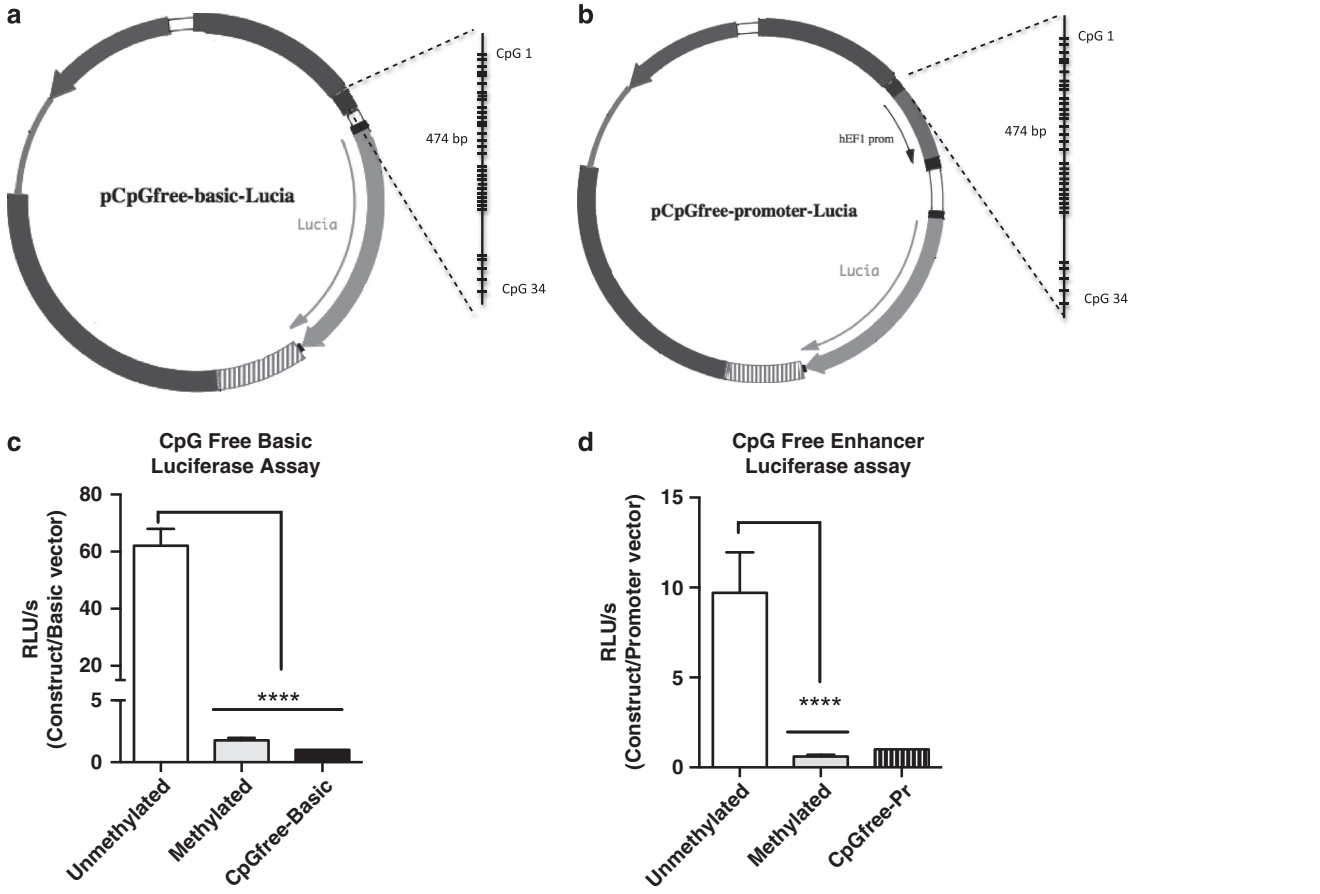

Figure 5. Promoter and enhancer properties repressed by DNA methylation in BEGAIN 474-bp amplicon. Schematic diagram of CpG-free lucia reporter vector with (**a**) no endogeneous promoter and (**b**) behind the human EF-1α promoter and placement of 474-bp insert into multiple cloning site. (**c**) The unmethylated insert shows promoter activity that is completely abolished by methylation (10 replicates per group, one-way ANOVA $F(2,27) = 106.8$, $P < 0.0001$, Tukey's *post hoc* $^{****}P < 0.0001$). (**d**) Placed in front of the promoter, the 474-bp insert showed enhancer activity again showing complete repression of activity by methylation (10 replicates per group, one-way ANOVA $F(2,23) = 17.80$, $P < 0.0001$, Holm–Sidak's *post hoc*, $^{****}P < 0.0001$).

were found in non-promoter regions where the relationship with expression is variable. We found many DMRs in gene bodies, where methylation is commonly associated with active transcription.[38] Our results are consistent with a regulatory mechanism for repressing transcription in these regions. For example, a reduction of gene body methylation can result in *de novo* histone modifications[39] that decrease transcription. As many of the DMRs in this study were found within gene bodies and intergenically, hypomethylation may result in gene repression.

Our study provides valuable information about often-overlooked regions of the genome.[40] In support of our findings, most variability in methylation occurs in gene bodies and intergenic regions, rather than promoters and upstream regulatory regions.[41] We identified two cluster regions, on chromosome 10 and the X chromosome, where DMRs fell primarily on short- and long-interspersed elements. DNA methylation maintains the stability of the genome by silencing these mobile elements.[42] Decreased methylation and increased expression of these elements could disrupt gene transcription. In addition, reduced methylation in these clusters could alter associated chromatin.[43] Moreover, four of the DMRs that we found within pericentromeric regions overlapped with over 20 ENCODE elements, representing regions under extensive epigenetic control. Abnormal methylation in these regions is implicated in developmental disorders,[44] suggesting important functional consequences.[45]

Among intragenic DMRs, we selected two according to significance for additional work: GRIK2 and BEGAIN. GRIK2 codes for glutamate ionotropic kainate receptor that is a ligand-gated cation channel. This channel is associated with gray and white matter astrocytes,[30] and altered calcium signaling in response to antidepressants.[32] *GRIK2* has been previously associated with psychiatric and neurological disorders,[30–32,46] including depression.[30–32] Our combined data showed that *GRIK2* is hypomethylated in intron 13 in cases as compared with controls, and we suspect that this intronic region of hypomethylation may influence alternative splicing of GRIK2,[47] potentially favoring the protein isoform with reduced permeability calcium signaling; however, additional work is required to explore this hypothesis.

BEGAIN, on the other hand, showed on average a threefold increase in methylation in cases, representing one of the strongest changes reported to date in psychiatric phenotypes. *BEGAIN* is poorly studied in humans but has been associated with diabetes and autoimmune disorders,[48] an interesting finding considering the growing evidence for the inflammatory basis of depression[49,50] and the role of astrocytes in the regulation of neuroinflammation.[51] In addition, a study in rats has shown increased *BEGAIN* expression in the frontal pole in response to prenatal stress as a paradigm for the etiology of schizophrenia.[52] BEGAIN is highly associated to the postsynaptic density proteins, and particularly to the postsynaptic density 95 (PSD95),[34,53,54] having

90% co-localization with PSD95,[53] and a role in sustaining the structure of this scaffolding protein.[55] PSD95 is the protein found in the postsynapic dendritic heads of excitatory synapses, and has been implicated in the coordination of the downstream communication of glutamate receptors, including GRIK2, through the binding of PSD95 to its guanylate kinase domains.[56] Recently, it has been shown that the astrocytes forming part of this excitatory synapse may have an important role in regulating the excitatory/inhibitory balance of neurons through PSD95.[57] The epigenetic alterations to *BEGAIN* and *GRIK2* and their association to astrocytically mediated PSD95 suggest possible defective synaptic communication and/or synaptic plasticity.[54]

Interestingly, our two top hits are involved in synaptic communication and regulation.[34,58] Whereas GRIK2 is known to be expressed in astrocytes and to be directly involved in astrocyte-mediated responses to antidepressant drugs,[31,32,46] *BEGAIN* has no known association to astrocytes. However, as the primary contribution of methylation was found in non-neuronal cells, it appears that astrocytes have a functional role in the regulation of this gene via methylation alterations. Otherwise, this would not be the first time that changes to genes in astrocytes at an epigenetic level are seen to influence normal neuronal function. For instance, Tao *et al.*[59] showed that selectively knocking-out Dicer in astrocytes leads to neuronal dysfunction and degeneration. Thus far BEGAIN has been investigated and localized in nuclei and synapses of neurons,[53] but there is no information on its relation to astrocytes. Much like GRIK2, BEGAIN could have an important role in both cell types. As BEGAIN is thought to maintain the structure of the postsynaptic density it would be interesting to see if the strong reduction of its transcript results in altered dendritic morphology as has become one of the emerging theories of autism, schizophrenia and Alzheimer's.[60] This study has opened the door to this and many other questions.

Our study is not without limitations. MBD2 has a higher affinity to densely methylated CpGs than antibody-based approaches; therefore, we may be missing single base-pair differences. Conversely, MBD2 is able to discriminate between 5′ hydroxymethylcytosine and 5′ methylcytosine[24] with greater efficiency than the monoclonal antibody directed against 5-methylcytidine.[61] Regarding our sample selection, altered transcription is often used as a marker for astrocytic dysfunction,[6,9,10] however, astrocyte dysfunction can be defined in many ways and may not be reflected by gene expression differences. Finally, we limited this study to DNA methylation changes and thus did not examine other epigenetic mechanism that may be involved in gene regulation. Despite these limitations, our study produced a list of DMRs showing clear evidence of astrocytic dysfunction in individuals who were depressed and died by suicide. Furthermore, we identified two genes involved in synaptic communication, *GRIK2* and *BEGAIN,* which appear to be regulated by DNA methylation in cases with astrocytic dysfunction. Each DMR identified here provides avenues for further investigation of the pathophysiological mechanisms underlying astrocytic dysfunction in mood disorders.

CONFLICT OF INTEREST

The authors declare no conflict of interest.

ACKNOWLEDGMENTS

We thank the members of the next-generation sequencing platform at Genome Quebec, and acknowledge the expert help of the DBCBB staff. CN is supported by a scholarship from the Fonds de recherche en Santé du Québec. CE is supported by the Canada Research Chairs program. NM is a Canadian Institutes of Health Research New Investigator and Bell Senior Fellow in Mental Health. GT is a national researcher from Fonds de recherche en Santé du Québec. This study was funded by a Canadian Institutes of Health Research operating grant (MOP# 119429).

REFERENCES

1 Kettenmann H, Ransom BR. *Neuroglia*. 2nd edn. Oxford University Press: New York, USA, 2005, xix, 601p.
2 Hercher C, Parent M, Flores C, Canetti L, Turecki G, Mechawar N. Alcohol dependence-related increase of glial cell density in the anterior cingulate cortex of suicide completers. *J Psychiatry Neurosci* 2009; **34**: 281–288.
3 Bernstein H-G, Steiner J, Bogerts B. Glial cells in schizophrenia: pathophysiological significance and possible consequences for therapy. *Exp Rev Neurother* 2009; **9**: 1059–1071.
4 Rajkowska G, Stockmeier CA. Astrocyte pathology in major depressive disorder: insights from human postmortem brain tissue. *Curr Drug Targets* 2013; **14**: 1225–1236.
5 Torres-Platas S, Hercher C, Davoli M, Maussion G, Labonté B, Turecki G *et al.* Astrocytic hypertrophy in anterior cingulate white matter of depressed suicides. *Neuropsychopharmacology* 2011; **36**: 2650–2658.
6 Ernst C, Nagy C, Kim S, Yang J, Deng X, Hellstrom I *et al.* Dysfunction of astrocyte connexins 30 and 43 in dorsal lateral prefrontal cortex of suicide completers. *Biol Psychiatry* 2011; **70**: 312–319.
7 Oberheim N, Goldman S, Nedergaard M. Heterogeneity of astrocytic form and function. *Methods Mol Biol* 2012; **814**: 23–45.
8 Sidoryk-Wegrzynowicz M, Wegrzynowicz M, Lee E, Bowman AB, Aschner M. Role of astrocytes in brain function and disease. *Toxic Pathol* 2011; **39**: 115–123.
9 Si X, Miguel-Hidalgo J, O'Dwyer G, Stockmeier C, Rajkowska G. Age-dependent reductions in the level of glial fibrillary acidic protein in the prefrontal cortex in major depression. *Neuropsychopharmacology* 2004; **29**: 2088–2096.
10 Choudary P, Molnar M, Evans S, Tomita H, Li J, Vawter M *et al.* Altered cortical glutamatergic and GABAergic signal transmission with glial involvement in depression. *Proc Natl Acad Sci USA* 2005; **102**: 15653–15658.
11 Bernard R, Kerman IA, Thompson RC, Jones EG, Bunney WE, Barchas JD *et al.* Altered expression of glutamate signaling, growth factor, and glia genes in the locus coeruleus of patients with major depression. *Mol Psychiatry* 2011; **16**: 634–646.
12 Turecki G, Ernst C, Jollant F, Labonte B, Mechawar N. The neurodevelopmental origins of suicidal behavior. *Trends Neurosci* 2012; **35**: 14–23.
13 Nagy C, Turecki G. Sensitive periods in epigenetics: bringing us closer to complex behavioral phenotypes. *Epigenomics* 2012; **4**: 445–457.
14 Dumais A, Lesage AD, Alda M, Rouleau G, Dumont M, Chawky N *et al.* Risk factors for suicide completion in major depression: a case-control study of impulsive and aggressive behaviors in men. *Am J Psychiatry* 2005; **162**: 2116–2124.
15 Arsenault-Lapierre G, Kim C, Turecki G. Psychiatric diagnoses in 3275 suicides: a meta-analysis. *BMC Psychiatry* 2004; **4**: 37.
16 Isometsa ET. Psychological autopsy studies--a review. *Eur Psychiatry* 2001; **16**: 379–385.
17 Sequeira A, Morgan L, Walsh DM, Cartagena PM, Choudary P, Li J *et al.* Gene expression changes in the prefrontal cortex, anterior cingulate cortex and nucleus accumbens of mood disorders subjects that committed suicide. *PloS ONE* 2012; **7**: e35367.
18 Kang H, Voleti B, Hajszan T, Rajkowska G, Stockmeier C, Licznerski P *et al.* Decreased expression of synapse-related genes and loss of synapses in major depressive disorder. *Nat Med* 2012; **18**: 1413–1417.
19 Goswami D, Jernigan C, Chandran A, Iyo A, May W, Austin M *et al.* Gene expression analysis of novel genes in the prefrontal cortex of major depressive disorder subjects. *Prog Neuropsychopharmacol Biol Psychiatry* 2012; **43C**: 126–133.
20 Underwood M, Kassir S, Bakalian M, Galfalvy H, Mann J, Arango V. Neuron density and serotonin receptor binding in prefrontal cortex in suicide. *Int J Neuropsychopharmacol* 2012; **15**: 435–447.
21 Kim S, Lee D. Prefrontal cortex and impulsive decision making. *Biol Psychiatry* 2011; **69**: 1140–1146.
22 Dent M, Segura-Anaya E, Alva-Medina J, Aranda-Anzaldo A. NeuN/Fox-3 is an intrinsic component of the neuronal nuclear matrix. *FEBS Lett* 2010; **584**: 2767–2771.
23 Li N, Ye M, Li Y, Yan Z, Butcher L, Sun J *et al.* Whole genome DNA methylation analysis based on high throughput sequencing technology. *Methods* 2010; **52**: 203–212.
24 Mellén M, Ayata P, Dewell S, Kriaucionis S, Heintz N. MeCP2 Binds to 5hmC enriched within active genes and accessible chromatin in the nervous system. *Cell* 2012; **151**: 1417–1430.
25 Tomilin N. Regulation of mammalian gene expression by retroelements and non-coding tandem repeats. *Bioessays* 2008; **30**: 338–348.

26 Koch C, Andrews R, Flicek P, Dillon S, Karaöz U, Clelland G *et al.* The landscape of histone modifications across 1% of the human genome in five human cell lines. *Genome Res* 2007; **17**: 691–707.
27 Thurman RE, Rynes E, Humbert R, Vierstra J, Maurano MT, Haugen E *et al.* The accessible chromatin landscape of the human genome. *Nature* 2012; **489**: 75–82.
28 Lehnertz B, Ueda Y, Derijck AA, Braunschweig U, Perez-Burgos L, Kubicek S *et al.* Suv39h-mediated histone H3 lysine 9 methylation directs DNA methylation to major satellite repeats at pericentric heterochromatin. *Curr Biol* 2003; **13**: 1192–1200.
29 Dejardin J. How chromatin prevents genomic rearrangements: locus colocalization induced by transcription factor binding. *Bioessays* 2012; **34**: 90–93.
30 Brand-Schieber E, Werner P. AMPA/kainate receptors in mouse spinal cord cell-specific display of receptor subunits by oligodendrocytes and astrocytes and at the nodes of Ranvier. *Glia* 2003; **42**: 12–24.
31 Li B, Zhang S, Li M, Zhang H, Hertz L, Peng L. Down-regulation of GluK2 kainate receptor expression by chronic treatment with mood-stabilizing anti-convulsants or lithium in cultured astrocytes and brain, but not in neurons. *Neuropharmacology* 2009; **57**: 375–385.
32 Li B, Zhang S, Zhang H, Hertz L, Peng L. Fluoxetine affects GluK2 editing, glutamate-evoked Ca(2+) influx and extracellular signal-regulated kinase phosphorylation in mouse astrocytes. *J Psychiatry Neurosci* 2011; **36**: 322–338.
33 Li H, Durbin R. Fast and accurate long-read alignment with Burrows-Wheeler transform. *Bioinformatics* 2010; **26**: 589–595.
34 Deguchi M, Hata Y, Takeuchi M, Ide N, Hirao K, Yao I *et al.* BEGAIN (brain-enriched guanylate kinase-associated protein), a novel neuronal PSD-95/SAP90-binding protein. *J Biol Chem* 1998; **273**: 26269–26272.
35 Weaver IC, Diorio J, Seckl JR, Szyf M, Meaney MJ. Early environmental regulation of hippocampal glucocorticoid receptor gene expression: characterization of intracellular mediators and potential genomic target sites. *Ann NY Acad Sci* 2004; **1024**: 182–212.
36 Labonte B, Yerko V, Gross J, Mechawar N, Meaney MJ, Szyf M *et al.* Differential glucocorticoid receptor exon 1(B), 1(C), and 1(H) expression and methylation in suicide completers with a history of childhood abuse. *Biol Psychiatry* 2012; **72**: 41–48.
37 Labonte B, Suderman M, Maussion G, Navaro L, Yerko V, Mahar I *et al.* Genome-wide epigenetic regulation by early-life trauma. *Arch Gen Psychiatry* 2012; **69**: 722–731.
38 Meissner A, Mikkelsen T, Gu H, Wernig M, Hanna J, Sivachenko A *et al.* Genome-scale DNA methylation maps of pluripotent and differentiated cells. *Nature* 2008; **454**: 766–770.
39 Hahn MA, Wu X, Li AX, Hahn T, Pfeifer GP. Relationship between gene body DNA methylation and intragenic H3K9me3 and H3K36me3 chromatin marks. *PloS ONE* 2011; **6**: e18844.
40 Gerstein M, Kundaje A, Hariharan M, Landt S, Yan K-K, Cheng C *et al.* Architecture of the human regulatory network derived from ENCODE data. *Nature* 2012; **489**: 91–100.
41 Consortium EP, Dunham I, Kundaje A, Aldred S, Collins P, Davis C *et al.* An integrated encyclopedia of DNA elements in the human genome. *Nature* 2012; **489**: 57–74.
42 Carnell AN, Goodman JI. The long (LINEs) and the short (SINEs) of it: altered methylation as a precursor to toxicity. *Toxicol Sci* 2003; **75**: 229–235.
43 Chueh AC, Northrop EL, Brettingham-Moore KH, Choo KH, Wong LH. LINE retrotransposon RNA is an essential structural and functional epigenetic component of a core neocentromeric chromatin. *PLoS Genet* 2009; **5**: e1000354.
44 Xu GL, Bestor TH, Bourc'his D, Hsieh CL, Tommerup N, Bugge M *et al.* Chromosome instability and immunodeficiency syndrome caused by mutations in a DNA methyltransferase gene. *Nature* 1999; **402**: 187–191.
45 Smith ZD, Meissner A. DNA methylation: roles in mammalian development. *Nat Rev Genet* 2013; **14**: 204–220.
46 Li B, Dong L, Fu H, Wang B, Hertz L, Peng L. Effects of chronic treatment with fluoxetine on receptor-stimulated increase of [Ca2+]i in astrocytes mimic those of acute inhibition of TRPC1 channel activity. *Cell Calcium* 2011; **50**: 42–53.
47 Wan J, Oliver VF, Zhu H, Zack DJ, Qian J, Merbs SL. Integrative analysis of tissue-specific methylation and alternative splicing identifies conserved transcription factor binding motifs. *Nucleic Acids Res* 2013; **41**: 8503–8514.
48 Wallace C, Smyth D, Maisuria-Armer M, Walker N, Todd J, Clayton D. The imprinted DLK1-MEG3 gene region on chromosome 14q32.2 alters susceptibility to type 1 diabetes. *Nat Genet* 2010; **42**: 68–71.
49 Miller AH, Maletic V, Raison CL. Inflammation and its discontents: the role of cytokines in the pathophysiology of major depression. *Biol Psychiatry* 2009; **65**: 732–741.
50 Raedler TJ. Inflammatory mechanisms in major depressive disorder. *Curr Opin Psychiatry* 2011; **24**: 519–525.
51 Kritz Jasna. Neuron-Astrocyte Interactions in Neuroinflammatin. In: Suzumura Akio KI (ed) *Neuron-Glia Interaction in Neuroinflammation*. Springer: New York, USA, 2013 pp, 75–90.
52 Kinnunen A, Koenig J, Bilbe G. Repeated variable prenatal stress alters pre- and postsynaptic gene expression in the rat frontal pole. *J Neurochem* 2003; **86**: 736–748.
53 Yao I, Iida J, Nishimura W, Hata Y. Synaptic and nuclear localization of brain-enriched guanylate kinase-associated protein. *J Neurosci* 2002; **22**: 5354–5364.
54 Xu W. PSD-95-like membrane associated guanylate kinases (PSD-MAGUKs) and synaptic plasticity. *Curr Opini Neurobiol* 2011; **21**: 306–312.
55 Deguchi M, Hata Y, Takeuchi M, Ide N, Hirao K, Yao I *et al.* BEGAIN (brain-enriched guanylate kinase-associated protein), a novel neuronal PSD-95/SAP90-binding protein. *J Biol Chem* 1998; **273**: 26269–26272.
56 Garcia E, Mehta S, Blair L, Wells D, Shang J, Fukushima T *et al.* SAP90 binds and clusters kainate receptors causing incomplete desensitization. *Neuron* 1998; **21**: 727–739.
57 Wang C-C, Chen P, Hsu C-W, Wu S-J, Lin C-T, Gean P. Valproic acid mediates the synaptic excitatory/inhibitory balance through astrocytes—a preliminary study. *Prog Neuropsychopharmacol Biol Psychiatry* 2012; **37**: 111–120.
58 Lerma J, Marques JM. Kainate receptors in health and disease. *Neuron* 2013; **80**: 292–311.
59 Tao J, Wu H, Lin Q, Wei W, Lu XH, Cantle JP *et al.* Deletion of astroglial Dicer causes non-cell-autonomous neuronal dysfunction and degeneration. *J Neurosci* 2011; **31**: 8306–8319.
60 Penzes P, Cahill M, Jones K, VanLeeuwen J-E, Woolfrey K. Dendritic spine pathology in neuropsychiatric disorders. *Nat Neurosci* 2011; **14**: 285–293.
61 Jin S-G, Kadam S, Pfeifer G. Examination of the specificity of DNA methylation profiling techniques towards 5-methylcytosine and 5-hydroxymethylcytosine. *Nucleic Acids Res* 2010; **38**: 11.

Supplementary Information accompanies the paper on the Molecular Psychiatry website (http://www.nature.com/mp)